

Deep polytopic autoencoders for low-dimensional linear parameter-varying approximations and nonlinear feedback controller design

Jan Heiland* Yongho Kim[†] Steffen W. R. Werner[‡]

**Department of Mathematics and Natural Sciences, Institute of Mathematics, Technische Universität Ilmenau, Germany.*

Email: jan.heiland@tu-ilmenau.de, ORCID: [0000-0003-0228-8522](https://orcid.org/0000-0003-0228-8522)

[†]*Max Planck Institute for Dynamics of Complex Technical Systems, Sandtorstraße 1, 39106 Magdeburg, Germany.* Email: ykim@mpi-magdeburg.mpg.de, ORCID: [0000-0003-4181-7968](https://orcid.org/0000-0003-4181-7968)

[‡]*Department of Mathematics and Division of Computational Modeling and Data Analytics, Academy of Data Science, Virginia Tech, Blacksburg, VA 24061, USA.*

Email: steffen.werner@vt.edu, ORCID: [0000-0003-1667-4862](https://orcid.org/0000-0003-1667-4862)

Abstract: Polytopic autoencoders provide low-dimensional parametrizations of states in a polytope. For nonlinear PDEs, this is readily applied to low-dimensional linear parameter-varying (LPV) approximations as they have been exploited for efficient nonlinear controller design via series expansions of the solution to the state-dependent Riccati equation. In this work, we develop a polytopic autoencoder for control applications and show how it improves on standard linear approaches in view of LPV approximations of nonlinear systems. We discuss how the particular architecture enables exact representation of target states and higher order series expansions of the nonlinear feedback law at little extra computational effort in the online phase and how the linear though high-dimensional and nonstandard Lyapunov equations are efficiently computed during the offline phase. In a numerical study, we illustrate the procedure and how this approach can reliably outperform the standard linear-quadratic regulator design.

Keywords: Nonlinear systems, nonlinear feedback control, parameter-varying approximations, Riccati equations, Lyapunov equations

Mathematics subject classification: 34H05, 37N35, 65F45, 76D55, 93B52

1 Introduction

The design of feedback controllers for nonlinear high-dimensional systems is a challenging task and there exists no generally applicable and computationally feasible approach. Here, we consider input-affine systems of the form

$$\dot{x}(t) = f(x(t)) + Bu(t), \quad y(t) = Cx(t), \quad (1)$$

where for time $t \geq 0$, $x(t) \in \mathbb{R}^n$ denotes the state, $u(t) \in \mathbb{R}^m$ and $y(t) \in \mathbb{R}^\ell$ denote the system's input and output, $f: \mathbb{R}^n \rightarrow \mathbb{R}^n$ is a possibly nonlinear function, and $B \in \mathbb{R}^{n \times m}$ and $C \in \mathbb{R}^{\ell \times n}$ are linear input and output operators represented as matrices. The general idea of feedback controller design is to identify a mapping $\mathcal{K}: x(t) \rightarrow u(t)$ so that with the choice of $u = \mathcal{K}(x)$, the system's state x and output y satisfy desired criteria. A typical application is feedback stabilization that seeks to achieve $x(t) \rightarrow 0$ as $t \rightarrow \infty$ or the more general task of *set-point control*, namely $x(t) \rightarrow x^*$ for some state $x^* \in \mathbb{R}^n$ that fulfills $f(x^*) = 0$.

For the controller design for systems of the form (1), methods like backstepping [34], feedback linearization [41, Chap. 5.3], and sliding mode control [22] require structural assumptions, whereas general approaches based on the Hamilton-Jacobi-Bellman (HJB) equations are only feasible for very moderate system sizes or in combination with model reduction; see, e.g., [16] for polynomial expansions, [23] for tensorized approximations, or [3] for an approach that addresses general PDEs based on first reducing the state-space dimension through, e.g., POD. Other efforts try to approximate the solution of the HJB equations by deep neural networks; see [20]. The commonly employed state-dependent Riccati equation (SDRE) approximation to the HJB equations (see, e.g., [18] for a survey) lifts a significant portion of the computational complexity. Nonetheless, this approach became available for large-scale systems only recently due to further simplifications; see [13] for a linear update scheme and [1] for approximations through series expansions for systems of a certain parametric structure. These structural assumptions have been lifted in our previous work (see [30]) so that, with the help of model reduction, now a large class of nonlinear control systems can be treated with series expansions of the SDRE.

The underlying idea is the approximation of the nonlinear system (1) through a very low-dimensional linear parameter-varying (LPV) system so that the series expansion of any nonlinear feedback law can be formulated with respect to a few parameters rather than the full state; see our previous works [21, 30] and related discussions in [1, 2]. In particular, the results in [30] indicate a measurable improvement of the nonlinear SDRE feedback over a related, well-tuned and robust linear-quadratic regulator (LQR) but left space for further performance improvements, for example, through

- (i) higher order expansions of the nonlinear feedback, or
- (ii) nonlinear parametrizations of the velocity states.

For higher order expansions of nonlinear feedback laws, a low-dimensional parametrization of the states is crucial since the number of coefficients grows drastically with the dimension of the parametrization and the order of the expansion so that both topics are linked to the single question if a nonlinear parametrization can provide sufficiently accurate low-dimensional approximations with only few degrees of freedom.

It is known that linear parametrizations like the (linearly) optimal approach of *proper orthogonal decomposition* (POD, see, e.g., [26]) have a natural limit on the approximation accuracy, which is commonly expressed through the Kolmogorov n -width; see [37]. Thus, there have been many efforts and positive results concerning the use of nonlinear model order reduction approaches including, for example, polynomial manifold maps [9, 17] or general nonlinear autoencoders [26, 38, 40]. An alternative for accurate low-dimensional parametrizations is found in the use of local bases [4]; see the recent works that consider local POD bases state reconstruction on subsets of the given dataset [5, 6, 33] or our previous work on local bases approximations via autoencoders [31, 32]. Basically, local bases are designed for subsets of states considered to have high similarities. However, local bases require a mechanism to identify the subsets and which basis is to be used.

Standard approaches use clustering for this purpose, for example, k -means clustering, fuzzy c -means clustering, and deep clustering [8, 24, 25].

In this work, we call on autoencoders with smooth basis selection and present a purely computational approach to design reduced-order parametrizations of nonlinear equations and provide algorithms and basic results for applications in nonlinear feedback control. Therefore, we extend our recently developed framework of polytopic autoencoders [32] that combines an autoencoder with the selection of local bases in terms of polytope vertices towards the use in set-point control. In particular, we directly impose the set-point condition $f(x^*) = 0$ onto the autoencoder so that we obtain a nonlinear encoding of very small dimension with arbitrary accuracy in the relevant part of the state space. To this end, we derive explicit expressions for the Jacobian of the decoder, which we then can exploit in theory and practice for analysis and synthesis of higher order expansions of the SDRE feedback. The precomputation of the expansion coefficients requires the solution of large-scale matrix-valued algebraic equations of a nonstandard form. Here, we call and expand on recent advances in the solution of indefinite matrix Lyapunov and Riccati equations; see [35, 39]. We note that the derived representation through a polytopic LPV system is suited for controller design on the base of linear matrix inequalities (LMIs); see, e.g., [7]. However, since the reduction only considers the structure but not the high-dimensional state space, the systems to solve are far too large for state-of-the-art LMI solvers. We exemplify the procedure and potentials of this general-purpose approach to nonlinear feedback design with a numerical example based on the two-dimensional flow past a cylinder.

The overall structure of this paper can be summarized as follows: We recall in Section 2 that a general nonlinear control system can be approximated by a low-dimensional LPV system, which can be exploited for controller design in particular if the parameter dependency itself is linear. In view of providing a performant but maximally low-dimensional parametrization, we resort to clustered polytopic autoencoders that encode the states of a dynamical system in a polytope and decode them with locally adapted bases; see Section 3. An interesting result in view of controller design is that this nonlinear decoding has a Taylor expansion with vanishing second-order terms (Lemma 1). For the actual controller design in Section 4, we consider series expansions of state-dependent Riccati equation. Here, we extend the formulas to consider nonlinear parameter dependencies and higher order terms in the expansion. We discuss and showcase, how the relevant large-scale matrix equations can be solved numerically. Finally, we report numerical experiments that illustrate the performance improvement of the polytopic autoencoder over standard approximation schemes that explore the different levels of approximation to the underlying nonlinear SDRE feedback design, and that investigate the gain in controller performance for a commonly considered flow control problem; see Section 6. As a result, we obtain a model-based nonlinear controller of reduced complexity, with the reduction tailored to snapshot data. The paper is concluded in Section 7.

2 Low-dimensional linear parameter-varying approximations

For nonlinear systems like (1), we consider *quasi*-LPV approximations of the form

$$\dot{x}(t) = A(\rho(x(t)))x(t) + Bu(t), \quad y(t) = Cx(t). \quad (2)$$

Such systems can be derived from an (exact) state-dependent coefficient representation such as $f(x) = \tilde{A}(x)x$ and a parametrization of the state $x(t) \approx \tilde{x}(t) = \nu(\mu(x(t)))$, where μ

is an encoder and ν is a decoder; see [30]. In this case, we set $\rho = \mu(x)$ and $A(\rho) := \tilde{A}(\nu(\rho))$. Note that the parameter ρ depends on the state, hence the term *quasi-LPV*.

Remark 1. In the example application of fluid flow models, the coefficient function \tilde{A} is readily available; cf. [28]. Here, the function \tilde{A} is linear so that a linear decoding will lead to linear parameter dependencies as they have been proven beneficial for controller design; see, e.g., [7].

In what follows, we refer by ρ_i to the i -th component of a vector-valued quantity ρ . To reduce the notation, we omit dependencies and sometimes write, e.g., ρ or $\rho(t)$ instead of $\rho(x(t))$. Furthermore, we will denote the *Kronecker product* by \otimes .

3 Polytopic parametrizations for control

In polytopic autoencoders (PAEs), the state is represented through generalized barycentric coordinates with respect to $R \in \mathbb{N}$ vertices $\{\tilde{x}_k\}_{k=1}^R \subset \mathbb{R}^n$ of a polytope; see, e.g., our previous work [32] for a more detailed introduction. As a polytope is bounded, one can always assume without loss of generality that the coordinates $\rho(t) \in \mathbb{R}^R$ in the reconstruction will be positive and sum up to one, i.e., for the $\tilde{x}(t)$ in the polytope it holds that

$$\tilde{x}(t) = \sum_{k=1}^R \rho_k(t) \tilde{x}_k, \quad \text{with } \rho(t) \geq 0 \text{ and } \sum_{k=1}^R \rho_k(t) = 1. \quad (3)$$

An immediate advantage of the polytopic parametrization for the intended controller design through series expansions results from the boundedness of the reconstruction, which keeps the controller gains bounded so that we can expect good approximations in series expansions while possible scaling issues will be detected when precomputing the expansion coefficients.

For the application in controller design, the consistency at the target state x^* is important. We note that a design like (3) is not capable of exactly parametrizing a target value $x^* = 0$ unless the vertices \tilde{x}_k come with a specific linear dependency. Moreover, for the intended series expansions around the target state, accuracy is guaranteed if $\|\rho(t)\|$ is small, which, however, contradicts the summation condition in (3). To address these two requirements, we include $\tilde{x}_0 = 0$ in the training of the reconstruction basis, where we impose the positivity and summation constraint on the ρ variable extended by ρ_0 , i.e.,

$$\rho_0(t) + \sum_{k=1}^R \rho_k(t) = 1. \quad (4)$$

This way, the tuple $(1, \rho(t)) = (1, 0) \in \mathbb{R}^{R+1}$ will be a feasible value in the extended parameter space that exactly represents the setpoint $x^* = 0 \in \mathbb{R}^n$. Moreover, smoothness in the parameter space, will ensure that ρ is small around the origin.

As for the use of local bases, we assume that q different polytopes with vertices

$$\{\tilde{x}_k^{(j)}\}_{k=1, \dots, R; j=1, \dots, q} \subset \mathbb{R}^n$$

are to be used as local bases for the reconstruction. Then, a direct implementation would compute both the local coordinates ρ and the index j of the relevant polytope and reconstruct according to the formula

$$\tilde{x} = \left[\tilde{x}_1^{(1)} \quad \dots \quad \tilde{x}_R^{(1)} \quad \tilde{x}_1^{(2)} \quad \dots \quad \tilde{x}_R^{(2)} \quad \dots \quad \tilde{x}_1^{(q)} \quad \dots \quad \tilde{x}_R^{(q)} \right] (\alpha \otimes \rho) \quad (5)$$

where, in this case, $\alpha = e_j$ is the j -th canonical basis vector. Instead of this *hard selection* of the j -th polytope, we rather use a smooth clustering network (e.g., [25, 43]) that blends between the polytopes by choosing $\alpha = c(\rho) \in \mathbb{R}^q$, with $c(\rho) \geq 0$ and $\sum_{\ell=1}^q c(\rho)_\ell = 1$. We note that the summation condition on $c(\rho)$ allows to consider $c(\rho) \otimes \rho$ as generalized barycentric coordinates in the polytope spanned by all vertices as in (5); see [32, Lem 3.1].

Under the preceding considerations, we propose a polytopic autoencoder designed for set-point control towards $x^* = 0$ that consists of the following three components:

- (i) A nonlinear encoder $\mu: \mathbb{R}^n \rightarrow \mathbb{R}^{r+1}$ so that

$$(\rho_0, \rho) = \mu(x) =: \text{softmax}(F_e(x) + e_1),$$

with a scalar function ρ_0 and $\rho(t) \in \mathbb{R}^r$, where $e_1 \in \mathbb{R}^{r+1}$ is the first unit vector and $F_e: \mathbb{R}^n \rightarrow \mathbb{R}^{r+1}$ is a nonlinear convolutional neural network described via

$$\begin{aligned} h_1 &= \mathbb{T}x, \\ h_2 &= \text{ELU}(\text{Conv}_1(h_1)), \\ &\vdots \\ h_L &= \text{ELU}(\text{Conv}_{L-1}(h_{L-1})), \\ F_e(x) &= \text{FC}(h_L). \end{aligned}$$

Here, \mathbb{T} denotes the interpolation of spatially distributed data onto a pixel grid as it is needed for the convolutions, ELU is the exponential linear unit (ELU) activation function [19], FC is a fully connected layer, and Conv_i is a convolutional layer, $i \in \{1, 2, \dots, L-1\}$ for some depth parameter $L \in \mathbb{N}$. Each layer is designed without bias terms to ensure $F_e(0) = 0$ so that with the *softmax function*

$$\text{softmax}(\xi)_i = \frac{\xi_i \tanh(10\xi_i)}{\sum_{j=1}^{r+1} \xi_j \tanh(10\xi_j)}$$

for $i = 1, \dots, r+1$ and $\xi = (\xi_1, \dots, \xi_{r+1}) \in \mathbb{R}^{r+1}$, we achieve, by design, that the output $(\rho_0(t), \rho(t))$ satisfies

$$(\rho_0(t), \rho_k(t)) \geq 0 \quad \text{and} \quad \rho_0(t) + \sum_{k=1}^r \rho_k(t) = 1;$$

and in particular $\mu(0) = (1, 0)$.

- (ii) A smooth clustering network $c: \mathbb{R}^r \rightarrow \mathbb{R}^q$, with

$$c(\rho) = \text{softmax}(F_c(\rho) + \hat{e}_1), \tag{6}$$

where \hat{e}_1 is the first unit vector in \mathbb{R}^q and

$$F_c(\rho) = \text{ELU}(\text{FC}(\rho)),$$

with no bias, i.e., $F_c(0) = 0$. By design, for the output $c(\rho)$, we have that

$$c(\rho(t)) \geq 0 \quad \text{and} \quad \sum_{i=1}^q c(\rho(t))_i = 1$$

hold, so that $(\rho_0, c(\rho) \otimes \rho)$ satisfies the positivity and summation conditions (4).

(iii) A trainable linear map $W \in \mathbb{R}^{n \times qr}$ that realizes the reconstruction (cf. (5)) as

$$\tilde{x} = W(c(\rho) \otimes \rho). \quad (7)$$

A few comments on the design of the autoencoder and motivation:

- Generally, the property that $F_e(0) = 0$ and $F_c(0) = 0$ can be achieved by using standard (convolutional) linear layers without bias terms and with any activation function that crosses the origin.
- The use of the extra ρ_0 variable ensures that ρ is zero at the origin despite being valid coordinates in a polytope.
- The smooth clustering network, as opposed to a standard clustering, also ensures differentiability of the network as it will become important for the series expansion.
- The design of the clustering network ensures that $c(0) = e_1$ so that values of ρ close to zero are associated with the first cluster and that $c(\mu(0)) \otimes \mu(0) = (1, 0) \in \mathbb{R}^{qr}$ represents the target vector $x^* = 0$ exactly.

With the following lemma, we summarize the resulting properties when employing the autoencoder in series expansions of the coefficient function.

Lemma 1. *Given the smooth clustering network c as defined in (6) and the corresponding LPV coefficient function*

$$\rho \rightarrow A(\rho) = \tilde{A}\left(W(c(\rho) \otimes \rho)\right) \quad (8)$$

defined through the linear map $\tilde{A}: \mathbb{R}^n \rightarrow \mathbb{R}^{n \times n}$ and the decoder (7). Then, it holds that

- (a) *the coefficient function (8) is differentiable,*
 (b) *the Jacobian of the clustering network c is zero at $\rho = 0$, i.e.,*

$$c'(\rho)|_{\rho=0} = 0 \in \mathbb{R}^{q,r},$$

and

- (c) *the second-order Taylor expansion of (8) coincides with the first-order expansion and reads*

$$A(\rho) \approx A(0) + \sum_j^r \rho_j \tilde{A}(w_j), \quad (9)$$

where w_j are the first r columns of $W \in \mathbb{R}^{n \times qr}$ as in (7).

Proof. As for the result (a), we note that, by construction, c is a concatenation of arbitrarily often differentiable functions. As for the part (b), by direct computations, we can confirm that $c'(F_c(\rho) + \hat{e}_1)|_{\rho=0} = c'(\hat{e}_1) = 0 \in \mathbb{R}^{q \times r}$.

Since the coefficient map

$$\rho \rightarrow \tilde{A}\left(W(c(\rho) \otimes \rho)\right)$$

is linear in components that concern W and \tilde{A} (cf. Equation (7) and Remark 1), we can reduce the argument to the nonlinear part $\rho \rightarrow c(\rho) \otimes \rho$. With $\rho = 0$, from

$$c(\rho + h) \otimes (\rho + h) - c(\rho) \otimes \rho = c(0 + h) \otimes h,$$

we derive the first and second-order expansion terms of the map $\rho \rightarrow c(\rho) \otimes \rho$ in the increment h at $\rho = 0$ as

$$c(0 + h) \otimes h = (c(0) + c'(0)h + \mathcal{R}(h)) \otimes h$$

with the remainder term $\mathcal{R}(h) \in o(|h|)$, meaning that \mathcal{R} approaches 0 faster than h itself. Thus, the second-order expansion of $\rho \rightarrow c(\rho) \otimes \rho$ around the origin 0 reads

$$c(\rho) \otimes \rho \approx c(0) \otimes \rho + (c'(0)\rho) \otimes \rho = c(0) \otimes \rho + (c'(0) \otimes I)(\rho \otimes \rho),$$

where $c'(0) \in \mathbb{R}^{q \times r}$ is the Jacobian of c at $\rho = 0$. With $c'(0) = 0$, the second-order terms vanish so that with $c(0) = \hat{e}_1$, the second-order expansions reduces to the first order approximation of the polytopic reconstruction that reads

$$\tilde{x}(\rho) \approx W(c(0) \otimes \rho) = W(\hat{e}_1 \otimes \rho) = W \begin{bmatrix} \rho \\ 0 \\ \vdots \\ 0 \end{bmatrix} = \sum_{j=1}^r \rho_j w_j.$$

Finally, formula (9) follows from the linearity of \tilde{A} and W . \square

Remark 2. We note the following consistency property in the smooth clustering. By construction, the first r columns of W describe the local basis for the reconstruction in the cluster associated with $\rho = 0$. Accordingly, the linearization around the origin only considers the basis that is associated with the origin.

4 Higher order series expansions of LPV approximations in SDRE feedback design

Although, as shown in Lemma 1, the second-order expansion of the coefficient function A coincides with the expansion of first order, the feedback law will still exhibit second-order dependencies as we will lay out in this section. For the *quasi*-LPV system (2), the nonlinear SDRE feedback design defines the input u as

$$u(t) = -B^T P(\rho(x(t)))x(t), \quad (10)$$

where $P(\rho)$ solves the SDRE

$$A(\rho)^T P(\rho) + P(\rho)A(\rho) - P(\rho)BB^T P(\rho) = -C^T C. \quad (11)$$

We note that for *quasi*-LPV systems the parameter changes continuously with the states. Since the repeated solve of (11) is costly, series expansions of the feedback law (10) have been proposed. We now briefly derive the formulas for higher order expansions of the solution to (11) with nonlinear parameter dependencies in A . For linear parameter dependencies, the first-order approximation has been developed in [10] for a single parameter dependency and has been extended in [1] to the multivariate case.

If the state dependency of the SDRE solution is parametrized through ρ , the multivariate Taylor expansion of P about $\rho_0 = 0$ up to order p reads

$$P(\rho) \approx P_0 + \sum_{1 \leq |\alpha| \leq p} \rho^{(\alpha)} P_\alpha, \quad (12)$$

where $\alpha = (\alpha_1, \dots, \alpha_r) \in \mathbb{N}^r$ is a multiindex with $|\alpha| := \sum_{i=1}^r \alpha_i$, where the coefficients are $\rho^{(\alpha)} := \rho_1^{\alpha_1} \rho_2^{\alpha_2} \dots \rho_r^{\alpha_r}$, and where, importantly, all P_α are constant symmetric matrices, namely

$$P_\alpha = \frac{1}{\alpha_1! \alpha_2! \dots \alpha_r!} \frac{\partial^{|\alpha|}}{\partial \rho_1^{\alpha_1} \partial \rho_2^{\alpha_2} \dots \partial \rho_r^{\alpha_r}} P(0).$$

We note that, because the function P is not known, this formula is merely stated to confirm that the P_α are constant matrices. Practically, in what follows, we will compute the P_α directly by equating coefficients in truncated series.

For the nonlinear parameter dependencies in $A(\rho)$, we will consider a truncated series expansion of A :

$$A(\rho) \approx A_0 + \sum_{1 \leq |\alpha| \leq p} \rho^{(\alpha)} A_\alpha, \quad (13)$$

where A_α are constant matrices; see (9) that describes the first and second-order expansions as follows: For $p = 1$, we can identify all $|\alpha| = p$ with $k = 1, \dots, r$ and obtain $\rho^{(\alpha)} A_\alpha = \rho_k \tilde{A}(w_k)$, where w_k is the k -th column of W . Following Lemma 1, in the considered case with the structure of the nonlinear decoding as $\rho \rightarrow W(c(\rho) \otimes \rho)$, the second-order expansion coincides with the first-order one. We also note that, if \tilde{A} is known (see Remark 1), then A_0 is readily inferred without knowledge of ρ or W .

We insert the expansions of A and P , namely (12) and (13), into the SDRE (11) and solve for the coefficients P_α by matching the individual powers of ρ . For $\alpha = 0$, we obtain the classical standard Riccati equation

$$A_0^\top P_0 + P_0 A_0 - P_0 B B^\top P_0 = -C^\top C, \quad (14)$$

as it is used for the design of feedback controllers for linear systems. Moving on, for $|\alpha| = 1$, the coefficients P_α are obtained from requiring that the first-order terms fulfill

$$P_0 \left(\sum_{|\alpha|=1} \rho^{(\alpha)} A_\alpha \right) + \left(\sum_{|\alpha|=1} \rho^{(\alpha)} A_\alpha \right)^\top P_0 - \sum_{|\alpha|=1} \rho^{(\alpha)} P_\alpha B B^\top P_0 - P_0 B B^\top \sum_{|\alpha|=1} \rho^{(\alpha)} P_\alpha = 0,$$

for arbitrary values of ρ . This defines the P_α as the solutions to the Lyapunov equations

$$\left(A_0 - B B^\top P_0 \right)^\top P_\alpha + P_\alpha \left(A_0 - B B^\top P_0 \right) = -A_\alpha^\top P_0 - P_0 A_\alpha, \quad (15)$$

for the r multiindices in $\alpha \in \mathbb{N}^r$ for which $|\alpha| = 1$ holds; see also [1, 30] where the same formulas have been derived. Similarly, we may obtain the P_α by setting the terms in which ρ appears quadratic to zero:

$$\begin{aligned} 0 = & P_0 \left(\sum_{|\alpha|=2} \rho^{(\alpha)} A_\alpha \right) + \left(\sum_{|\alpha|=1} \rho^{(\alpha)} P_\alpha \right) \left(\sum_{|\alpha|=1} \rho^{(\alpha)} A_\alpha \right) + \left(\sum_{|\alpha|=2} \rho^{(\alpha)} P_\alpha \right) A_0 + \dots \\ & - \left(\sum_{|\alpha|=1} \rho^{(\alpha)} P_\alpha \right) B B^\top \left(\sum_{|\alpha|=1} \rho^{(\alpha)} P_\alpha \right) - \left(\sum_{|\alpha|=2} \rho^{(\alpha)} P_\alpha \right) B B^\top P_0 - \dots, \end{aligned}$$

where the terms omitted via \dots stand for the transposed counterparts. Let α^* be a multiindex with $|\alpha^*| = 2$ and let β^* and δ^* be those two multiindices with $|\beta^*| = |\delta^*| = 1$

that satisfy $\beta^* + \delta^* = \alpha^*$. Then, the coefficient P_{α^*} that cancels the corresponding contributions in the equation above is defined as the solution to the Lyapunov equation

$$\begin{aligned} & (A_0 - BB^\top P_0)^\top P_{\alpha^*} + P_{\alpha^*} (A_0 - BB^\top P_0) \\ &= -P_0 A_{\alpha^*} - A_{\alpha^*}^\top P_0 - P_{\beta^*} A_{\delta^*} - A_{\delta^*}^\top P_{\beta^*} - P_{\delta^*} A_{\beta^*} \\ & \quad - A_{\beta^*}^\top P_{\delta^*} + P_{\beta^*} BB^\top P_{\delta^*} + P_{\delta^*} BB^\top P_{\beta^*}. \end{aligned} \quad (16)$$

Note that for given r and p , there exist exactly $\binom{r+p-1}{p}$ unique such multiindices α such that $|\alpha|=p$.

Finally, we note that for such a series expansion of P , the feedback law (10) reads

$$u(t) = -B^\top \left(\sum_{|\alpha| \leq p} \rho^{(\alpha)} P_\alpha \right) x(t) =: u_{P_{|\alpha| \leq p}}(t), \quad (17)$$

which with the precomputed $B^\top P_\alpha$ is efficiently evaluated by adapting the values of ρ . We also note that for $p = 0$, this formula reduces to the standard *linear quadratic regulator* (LQR) feedback with respect to a linearization about $x^* = 0$.

5 Solving the high-dimensional matrix equations

To compute the solutions to the occurring high-dimensional matrix equations (14)–(16), some reformulations and state-of-the-art approaches are needed. In the considered setup, we can exploit that the ranks of B and C are much smaller than the state-space dimension n and that A_0 in (13) is sparsely populated, so that the first equation (14)—a standard Riccati equation—can be efficiently solved for a low-rank approximation of the symmetric positive semi-definite stabilizing solution $Z_0 Z_0^\top \approx P_0$, with $Z_0 \in \mathbb{R}^{n \times k}$ and $k \ll n$; see [11, 42], e.g., via the low-rank Newton-Kleinman iteration [14, 39], the incremental subspace iteration [36] or the RADI method [12, 15].

However, for the two types of Lyapunov equations (15) and (16) occurring through the series expansion, some reformulations are needed to compute the solutions in this large-scale setting; namely, the right-hand sides need to be reformulated into symmetric low-rank factorizations. Given the approximation $Z_0 Z_0^\top \approx P_0$ of the initial Riccati equation (14), the right-hand side in (15) can be rewritten as

$$-A_\alpha^\top P_0 - P_0 A_\alpha \approx - \begin{bmatrix} A_\alpha^\top Z_0 & Z_0 \end{bmatrix} J \begin{bmatrix} Z_0^\top A_\alpha \\ Z_0^\top \end{bmatrix}, \quad (18)$$

where the symmetric yet indefinite center matrix is given by $J = \begin{bmatrix} 0 & I_k \\ I_k & 0 \end{bmatrix}$, with I_k denoting the k -dimensional identity matrix and k being the number of columns of Z_0 . For Lyapunov equations (15) with such symmetric factorized right-hand sides (18), the ADI approach has been extended to compute appropriate solution approximations of the form $L_\alpha D_\alpha L_\alpha^\top \approx P_\alpha$ following the format of the right-hand side; see [35]. Furthermore, while the coefficient matrix in (15), namely

$$A - BB^\top P_0 = A - BV^\top \quad (19)$$

with $V = B^\top P_0 \in \mathbb{R}^{n \times m}$, is dense and high-dimensional, it is not necessary to assemble this matrix at any point because (19) is a large-scale sparse matrix with low-rank

perturbation. Solution methods for large-scale Lyapunov equations only rely on matrix-vector operations or the solution to linear systems with (19). The latter can be efficiently computed using the Sherman-Morrison-Woodbury matrix inversion formula or augmented matrix approach [27] such that only the solution of linear systems with large-scale sparse coefficient matrices and matrix-vector products are needed. It is important to observe that the coefficient (19) is Hurwitz, i.e., all eigenvalues lie in the left open half-plane, such that the established solution methods can be applied.

Similarly, we can derive for the right-hand side of (16) symmetric indefinite low-rank factorizations of the form LDL^\top . Thereby, the factor are

$$L^\top = \begin{bmatrix} Z_0^\top A_{\alpha^*} \\ Z_0^\top \\ L_{\beta^*}^\top (A_{\delta^*} - BK_{\delta^*}) \\ L_{\delta^*}^\top (A_{\beta^*} - BK_{\beta^*}) \\ L_{\beta^*}^\top \\ L_{\delta^*}^\top \end{bmatrix}, \quad (20)$$

and

$$D = \begin{bmatrix} J & 0 & 0 & 0 & 0 \\ 0 & 0 & 0 & D_{\beta^*} & 0 \\ 0 & 0 & 0 & 0 & D_{\delta^*} \\ 0 & D_{\beta^*} & 0 & 0 & 0 \\ 0 & 0 & D_{\delta^*} & 0 & 0 \end{bmatrix}, \quad (21)$$

where we have the approximations of the solutions to the Lyapunov equations (15) as $L_{\beta^*} D_{\beta^*} L_{\beta^*}^\top \approx P_{\beta^*}$ and $L_{\delta^*} D_{\delta^*} L_{\delta^*}^\top \approx P_{\delta^*}$, and the intermediate feedback matrices $K_{\beta^*} = B^\top P_{\beta^*}$ and $K_{\delta^*} = B^\top P_{\delta^*}$. As for (15), this reformulation of the constant terms of (16) allows the application of the same computational procedures for the solution, for example, the LDL^\top -factorized ADI method [35]. The coefficient matrix in (16) is the same as in (15) such that it has the same properties being sparse plus low-rank and Hurwitz. Therefore, we can apply the same numerical approaches to solve (16) as for (15).

In both cases of Lyapunov equations (15) and (16), we have that the inner dimensions of the reformulated right-hand side terms (18), (20), and (21) depend on dimensions of the factors of the solution approximations to (14) and (15). Therefore, we can expect the dimensions of the right-hand side factors to be larger than the dimensions of the input and output matrices used in the Riccati equation (14). In general, we strongly recommend to compress the right-hand side factors at least to their numerical rank using economy-size QR and eigenvalue decompositions. All right-hand sides of Lyapunov equations considered in this paper can be written as indefinite symmetric factorizations of the form LDL^\top , with $L \in \mathbb{R}^{n \times k}$ and $D \in \mathbb{R}^{k \times k}$ symmetric. For the compression, first, compute the economy-size QR of $L = QR$, with $Q \in \mathbb{R}^{n \times k}$ and $R \in \mathbb{R}^{k \times k}$. Next, compute the eigenvalue decomposition of the symmetric matrix

$$RDR^\top = U\Lambda U^\top, \quad (22)$$

where $\Lambda \in \mathbb{R}^{k \times k}$ is a diagonal matrix of real eigenvalues and $U \in \mathbb{R}^{k \times k}$ is the matrix of the corresponding orthogonal eigenvectors. Next, the numerical rank is determined based on the diagonal matrix Λ . A typical choice here is to truncate all eigenvalues λ_i that are small in absolute value, e.g.,

$$|\lambda_i| < k \cdot \max_{i=1, \dots, k} |\lambda_i| \cdot \epsilon,$$

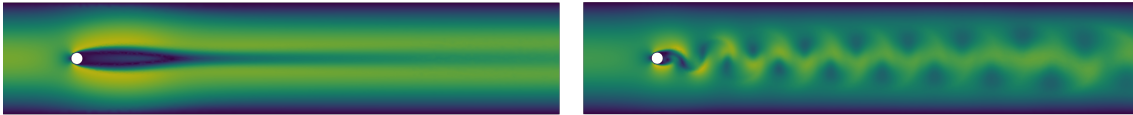


Figure 1: Spatial domain and snapshots of the flow behind a cylinder in the unstable steady state (left) and in the periodic vortex shedding regime (right); cf. [30].

where ϵ is the machine precision. Note that the original matrix D is assumed to be indefinite such that large positive as well as negative eigenvalues may occur, which need to be kept in the compression. For simplicity, assume that the eigenvalues in Λ are ordered by absolute size such that we have

$$\Lambda = \begin{bmatrix} \Lambda_1 & 0 \\ 0 & \Lambda_2 \end{bmatrix} \quad \text{and} \quad U = [U_1 \quad U_2],$$

where Λ_1, U_1 contain the eigenvalues and eigenvectors that remain and Λ_2, U_2 contain the eigenvalues and eigenvectors that are truncated. This results in the compression

$$LDL^T \approx QU_1\Lambda_1U_1^TQ^T = \tilde{L}\tilde{D}\tilde{L}^T,$$

where $\tilde{L} = QU_1$ and $\tilde{D} = \Lambda_1$, which is used to compute the solution to the matrix equations (15) and (16) instead of the original right-hand sides.

6 Numerical experiments

The code, data and results of the numerical experiments presented here can be found at [29].

6.1 Numerical setup

For comparability reasons, we consider here the same problem, numerical setup, and the same data points for training the models as in [30]. In short, the flow control problem of stabilizing the unstable steady-state of the flow behind a cylinder is modeled through the difference of the velocity v to the steady-stated and observed through outputs $y = Cx$. It is determined by the semi-discrete Navier-Stokes equations

$$M\dot{x} = N(x)x + Bu, \quad y = Cx, \quad x(0) = 0 \in \mathbb{R}^n, \quad (23)$$

written in so-called *divergence-free* coordinates of the difference state x , with $N: x(t) \rightarrow N(x(t)) \in \mathbb{R}^{n \times n}$ modeling the discrete diffusion-convection operator and $C \in \mathbb{R}^{6 \times n}$ and $B \in \mathbb{R}^{n \times 2}$ the discrete observation and control operators; cf. [30]. See also Figure 1 for a picture of the spatial domain and two snapshots of the flow behind a cylinder showing the flow velocities in the unstable steady state and with the periodic vortex shedding behavior. In the considered setup, the *Reynolds number* is set to 60 and the dimension of the spatially discretized model to $n = 51\,194$. For the time integration, a semi-explicit Euler scheme is employed, which treats the feedback and the nonlinearity explicitly.

We consider the steady-state solution as target state and aim for the stabilization of the difference system (23). To trigger instabilities and to collect training data, a test input

$$u(t) = [\sin(t) \quad 0]^T, \quad (24)$$

Table 1: Model complexity of the different PAE schemes and POD: # stands for *number of*. We distinguish between linear (lin.) and nonlinear (nonl.) mappings in the encoding and decoding.

Hyperparameters \ Scheme	POD-5	PAE-1.5	PAE-3.5	PAE-3.5 (p=1)
reduced dimension r	5	5	5	5
#clusters q	1	1	3	3
#encoding parameters	255970	42810	42810	42810
#encoding layers	1(lin.)	16(nonl.)	16(nonl.)	16(nonl.)
#decoding parameters	255970	255970	15+767910	255970
#decoding layers	1	1	1(nonl.)+1(lin.)	1

 Table 2: Average of the reconstruction errors (scaled with 10^3) of POD- r and PAE- $q.r$ on the time range $[0, 0.5]$ used for training.

Scheme \ r	2	3	4	5	6	7	8
POD- r	1.340	0.610	0.305	0.149	0.076	0.038	0.020
PAE-1. r	1.335	0.614	0.326	0.181	0.118	0.121	0.087
PAE-3. r	0.189	0.135	0.104	0.066	0.075	0.097	0.079
PAE-3. r (p=1)	17.670	7.501	5.217	5.628	2.745	6.794	2.307

is applied. We choose a deep convolutional encoder with depthwise separable convolutions to cope with the high computational complexity and memory requirements in this rather high-dimensional setup; see [32] for details. As a result the model complexity in terms of parameters that define the encoder and decoder can be lower than for, say, a comparable POD reduction; see Table 1. For training the PAEs, we adopt a semi-supervised learning methodology with the loss function

$$\mathcal{L}(v^{(i)}) := \lambda \|\tilde{x}^{(i)} - x^{(i)}\|_M - \ell(\rho^{(i)}) \cdot \log(c(\rho^{(i)})),$$

where $x^{(i)}$ is the i -th data point, $\rho^{(i)} := \mu(x^{(i)})$ and $\tilde{x}^{(i)} := \nu(\rho^{(i)})$ for the corresponding encoder and decoder μ and ν , where ℓ assigns labels that were precomputed by k -means clustering in \mathbb{R}^r , and where $\lambda > 0$ is a weighting factor between the reconstruction error (measured in the M -weighted L^2 -norm) and the clustering error. We note that the chosen *cross-entropy* loss is commonly used to smoothly assign labels and that the labeling ℓ is defined such that the target $\rho^* = 0$ is assigned to the first cluster. As it is standard practice, the loss is computed as the average over a *batch* of data points. Here, we consider 401 data points equally distributed in the time interval $[0, 0.5]$ as training data, and we use the *Adam optimizer* with learning rate 0.005, 3200 epochs, a batch size of 64 and the loss weight $\lambda = 100$.

6.2 Reconstruction errors

We evaluate the reconstruction performance of the PAE in the averaged M -norm error

$$\frac{1}{N} \sum_{i=1}^N \|x^{(i)} - \tilde{x}^{(i)}\|_M,$$

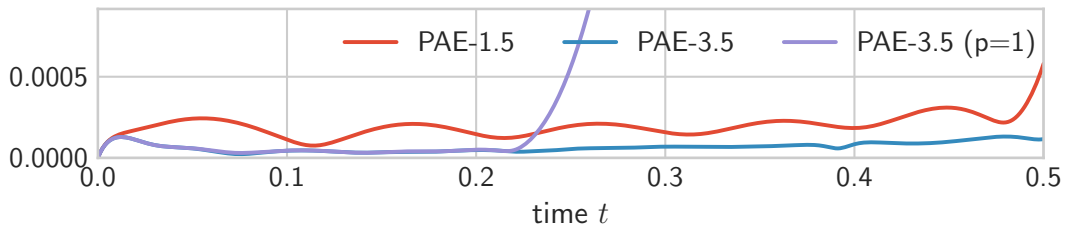


Figure 2: Trajectory with pointwise reconstruction errors $\|x(t^{(i)}) - \tilde{x}(t^{(i)})\|_M$. The improvement of using 3 clusters is clearly visible as is the initial alignment with the nonlinear approach PAE-3.5 (and the subsequent deviation from it) of the first-order expansion.

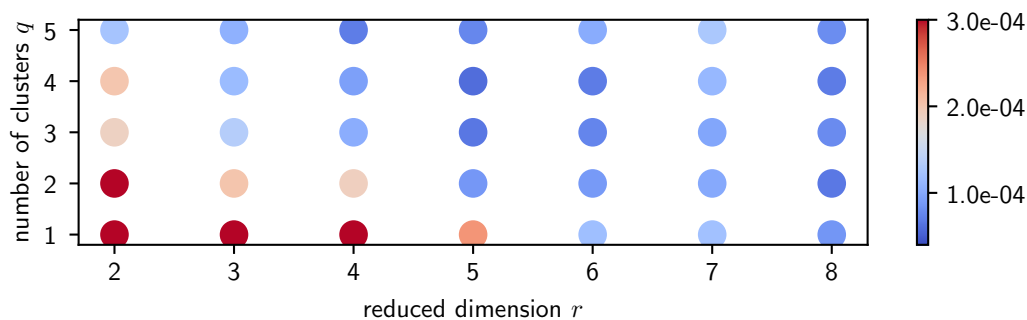


Figure 3: Grid search for the selection of r and q with lowest averaged reconstruction error. A trade-off between the number of clusters and the reduced dimension becomes clearly visible.

where $x^{(i)}$ is the i -th data point and $\tilde{x}^{(i)} = \nu(\mu(x^{(i)}))$ for the corresponding encoder and decoder μ and ν . As laid out in Table 2, the PAE-1.5 is comparable to the standard linear approach of POD for low dimensions $r = 2, 3, 4$, whereas the nonlinear encoding through the cluster selection significantly improves the reconstruction in low dimensions. As for the series expansion of the control law, only the first-order approximation is relevant, we tabulate this reconstruction error as well. Note that the bad average performance is due to the strong deviation for larger t , i.e., larger values of ρ , whereas for small t , the first-order approximation closely aligns with the nonlinear approach; see Figure 2.

Before turning to the controller design, we use a grid search to identify a suitable parameter setup for the reduced-order LPV approximation. As shown in Figure 3, the pair $(q, r) = (4, 5)$ achieves the lowest reconstruction error in the considered domain. Nonetheless, we selected $(q, r) = (3, 5)$ as a compromise of both accuracy and complexity.

6.3 SDRE approximation through series expansions

We check the approximation of the SDRE feedback along the example trajectory x generated by the test input (24). For that we compute the true SDRE feedback

$$u_P(t) = -B^T P(x(t))x(t),$$

where P solves the SDRE, and compare to $u_{\tilde{P}}$ and $u_{P_{|\alpha| \leq p}}$ that denote the feedback computed through the LPV approximation in (11) (via PAE- q .5, $q = 1, 3$) and the expansions (17) for $p = 0, 1, 2$, respectively. The data in Figure 4 shows that the LPV

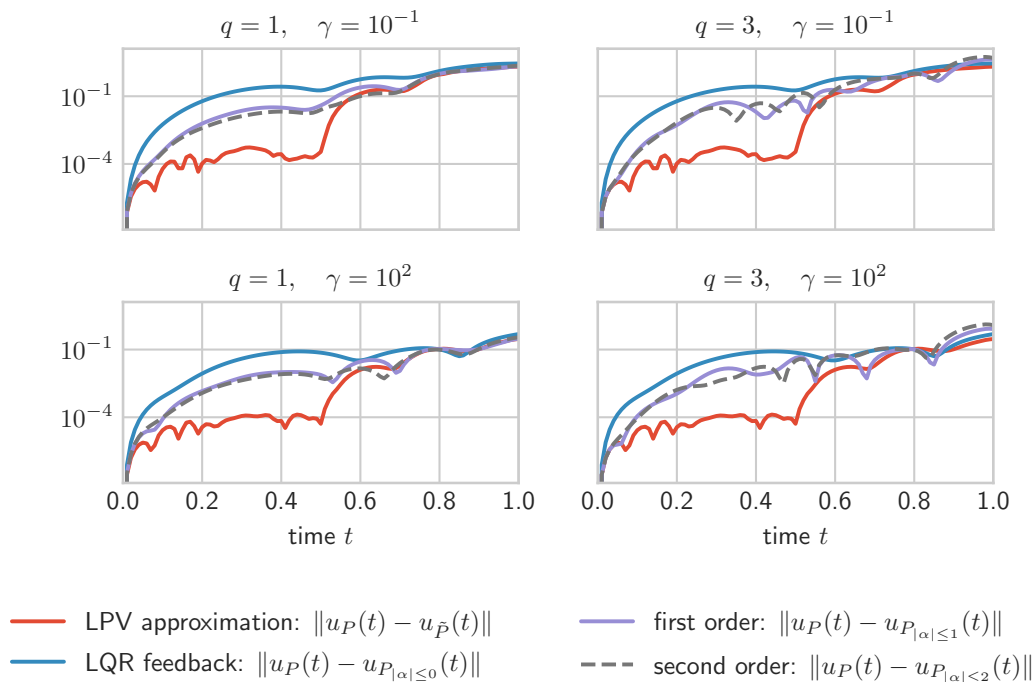


Figure 4: Differences to the exact SDRE feedback along a sample trajectory for feedback approximations through the LPV approximation of the nonlinearity by PAE-q.5, for $q = 1, 3$, and the corresponding zeroth, first and second-order series expansions of the SDRE feedback. The LPV approximation provides the most accurate approximation to the true SDRE feedback in its training regime up to 0.5. The first and second-order approximations also strongly improve over the classical LQR feedback.

approximation works particularly well for $t \leq 0.5$, which is the training regime, and that the first and second-order expansions significantly improve the zero-order approximation, which would be the LQR gain, but with a slight effect of the additional second-order terms.

6.4 Feedback performance

To evaluate the performance of the approximations for the controller design, we simulate the closed loop system with varying the two parameters $\gamma \in \{100, 10, 1, 0.1, 0.001\}$ that stands for the penalization factor of u in the underlying quadratic cost functional and the startup time $t_s > 0$ that marks the time after which the test input is turned off and the feedback is applied. In other words, γ is a parameter that weighs on the magnitude of the control and t_s regulates how far the system is deferred from the target state when the controller is activated. In Figure 5, for different orders $p = 0, 1, 2$ of approximation, we plot the averaged measured feedback magnitude

$$\frac{1}{t_e} \left(\int_{t_s}^{t_e} \|B^T \left(\sum_{|\alpha| \leq p} \rho(x(t))^{(\alpha)} P_\alpha \right) x(t)\|^2 dt \right)^{\frac{1}{2}}, \quad (25)$$

that tends to 0 for $t_e \rightarrow \infty$ if stabilization is achieved, and that is finite if and only if the simulation has not blown up before a finite end time t_e .

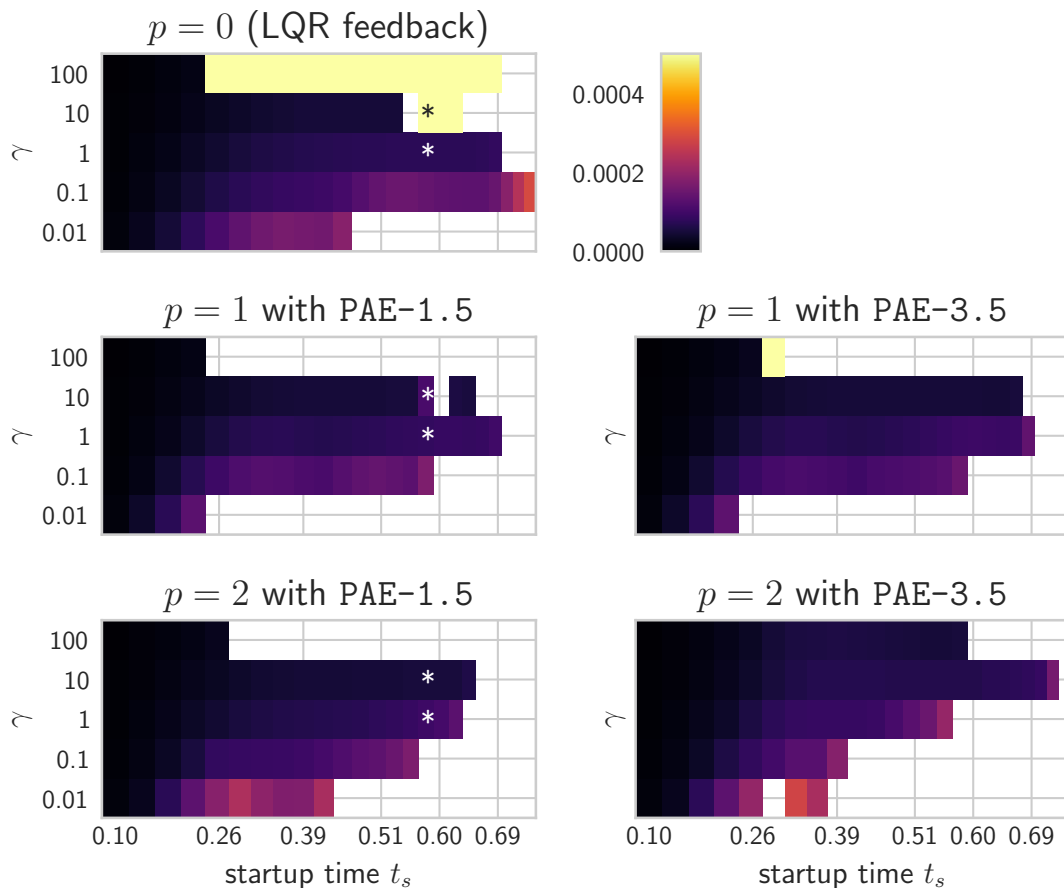


Figure 5: Performance index (25) map of the linear and nonlinear feedbacks for PAE reduced-order models with $r = 5$, $q = 1, 3$, the SDRE feedback law expansion (17) for $p = 0, 1, 2$ and varying penalization parameter γ and startup times t_s . The darker the color, the smaller (i.e., the better) the performance index. At the blank spaces, the system blew up. The trajectories of the data marked with * are plotted in Figure 6.

We plot the values of the performance index (25) for $t_e = 7.5$ and for various approximations to the nonlinear SDRE feedback in Figure 5 and the trajectories of selected cases in Figure 6. As we have observed before, the $p = 0$ expansion in (17), i.e., the LQR feedback, is remarkably performant for the optimal choice of the *Tikhonov* parameter γ . However, considering higher order expansions with $p = 1, 2$ together with the option to adapt the underlying approximation scheme, significantly widens the domain of attraction and can ensure reliable performance in particular for larger values of γ ; see, e.g., Figure 6 (top row) for the trajectory data for a setup with $\gamma = 10$, where only the second-order expansion achieves stabilization. The reason might be that a larger γ seeks for small (in magnitude) control actions, which makes better adaptation pay off while it reduces overshoots that may destabilize the nonlinear controller.

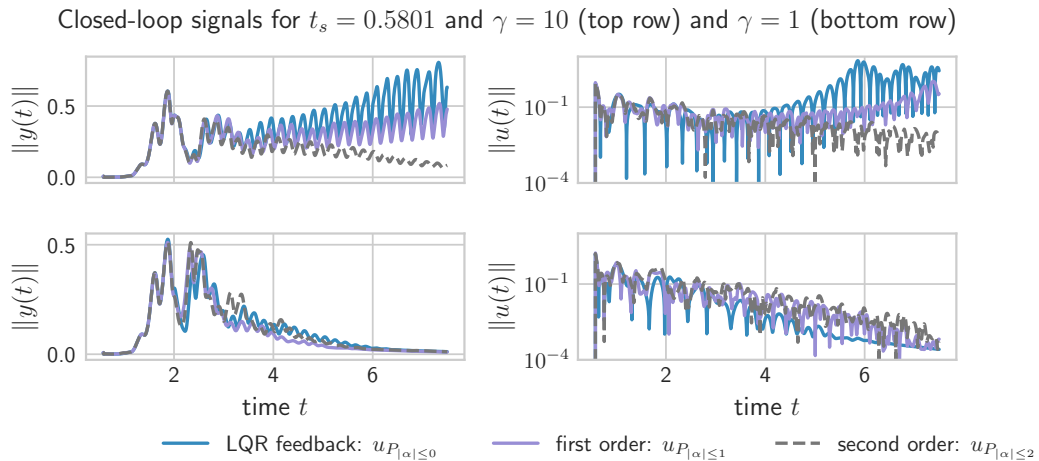


Figure 6: Measured output and feedback input signals for the distinguished data points from Figure 5. The second-order LPV approximation is capable of stabilizing the nonlinear system in situations, in which the first-order approximation begins to fail.

7 Conclusion

In this work, we considered the use of deep polytopic autoencoders and state-dependent Riccati equations for the design of nonlinear controllers. We use the concept of linear parameter-varying approximations of nonlinear dynamical systems that are parametrized by deep polytopic autoencoders, and we show that by the particular choice of autoencoders, the parametrization is differentiable and has vanishing second-order terms. For the nonlinear feedback design, we extend the series expansion of state-dependent Riccati equations to second-order terms for which we provide computable expressions in form of indefinite Lyapunov and Riccati equations. Finally, we test the proposed framework on the classical control example modeling the flow past a cylinder.

The proposed nonlinear autoencoder with smooth clustering significantly improves the parametrization quality at very low dimensions. For controller design, we established that for second-order expansions of the state-dependent feedback law, only the first-order expansions of the reduced-order linear parameter-varying coefficient are relevant, which reduces the computational effort by large. Regarding the performance of the resulting feedback, the overall picture is diffuse. While the linear quadratic regulator approach, for suitable weight parameters, ensured stability also well away from the origin, the nonlinear feedback design based on different approximation schemes, clearly extended the basin of attraction. As the choice of the approximation was solely based on a single open-loop simulation in a time range that did not cover the full range of the closed-loop simulation, in future work, we expect to gain additional performance by optimizing the approximation in view of feedback control.

Acknowledgments

Parts of this work have been carried out while Jan Heiland was with the Max Planck Institute for Complex Technical Systems, Magdeburg, and with the Otto von Guericke University Magdeburg.

Jan Heiland and Yongho Kim were supported by the German Research Foundation

(DFG) Research Training Group 2297 “Mathematical Complexity Reduction (MathCoRe)”, Magdeburg. Steffen W. R. Werner acknowledges Advanced Research Computing (ARC) at Virginia Tech for providing computational resources and technical support that have contributed to the results reported within this paper.

References

- [1] A. Alla, D. Kalise, and V. Simoncini. State-dependent Riccati equation feedback stabilization for nonlinear PDEs. *Adv. Comput. Math.*, 49(1):9, 2023. doi:10.1007/s10444-022-09998-4.
- [2] A. Alla and A. Pacifico. A POD approach to identify and control PDEs online through state dependent Riccati equations. e-print 2402.08186, arXiv, 2024. Optimization and Control (math.OC). doi:10.48550/arXiv.2402.08186.
- [3] A. Alla and L. Saluzzi. A HJB-POD approach for the control of nonlinear PDEs on a tree structure. *Appl. Numer. Math.*, 155:192–207, 2020. doi:10.1016/j.apnum.2019.11.023.
- [4] D. Amsallem, M. J. Zahr, and C. Farhat. Nonlinear model order reduction based on local reduced-order bases. *Int. J. Numer. Methods Eng.*, 92(10):891–916, 2012. doi:10.1002/nme.4371.
- [5] David Amsallem and Bernard Haasdonk. PEBL-ROM: Projection-error based local reduced-order models. *Adv. Model. Simul. Eng. Sci.*, 3(1), 2016. doi:10.1186/s40323-016-0059-7.
- [6] David Amsallem, Matthew J. Zahr, and Charbel Farhat. Nonlinear model order reduction based on local reduced-order bases. *Int. J. Numer. Methods Eng.*, 92(10):891–916, 2012. doi:doi.org/10.1002/nme.4371.
- [7] P. Apkarian, P. Gahinet, and G. Becker. Self-scheduled H_∞ control of linear parameter-varying systems: a design example. *Automatica*, 31(9):1251–1261, 1995. doi:10.1016/0005-1098(95)00038-X.
- [8] David Arthur and Sergei Vassilvitskii. K-means++: The advantages of careful seeding. In *Proceedings of the Eighteenth Annual ACM-SIAM Symposium on Discrete Algorithms*, pages 1027–1035, 2007. doi:10.5555/1283383.1283494.
- [9] J. Barnett and C. Farhat. Quadratic approximation manifold for mitigating the Kolmogorov barrier in nonlinear projection-based model order reduction. *J. Comput. Phys.*, 464:111348, 2022. doi:10.1016/j.jcp.2022.111348.
- [10] S. C. Beeler, H. T. Tran, and H. T. Banks. Feedback control methodologies for nonlinear systems. *J. Optim. Theory Appl.*, 107(1):1–33, 2000. doi:10.1023/A:1004607114958.
- [11] P. Benner and Z. Bujanović. On the solution of large-scale algebraic Riccati equations by using low-dimensional invariant subspaces. *Linear Algebra Appl.*, 488:430–459, 2016. doi:10.1016/j.laa.2015.09.027.
- [12] P. Benner, Z. Bujanović, P. Kürschner, and J. Saak. RADI: a low-rank ADI-type algorithm for large scale algebraic Riccati equations. *Numer. Math.*, 138(2):301–330, 2018. doi:10.1007/s00211-017-0907-5.

- [13] P. Benner and J. Heiland. Exponential stability and stabilization of extended linearizations via continuous updates of Riccati-based feedback. *Int. J. Robust Nonlinear Control*, 28(4):1218–1232, 2018. doi:10.1002/rnc.3949.
- [14] P. Benner, M. Heinkenschloss, J. Saak, and H. K. Weichelt. An inexact low-rank Newton-ADI method for large-scale algebraic Riccati equations. *Appl. Numer. Math.*, 108:125–142, 2016. doi:10.1016/j.apnum.2016.05.006.
- [15] C. Bertram and H. Faßbender. On a family of low-rank algorithms for large-scale algebraic Riccati equations. *Linear Algebra Appl.*, 687:38–67, 2024. doi:10.1016/j.laa.2024.01.020.
- [16] T. Breiten, K. Kunisch, and L. Pfeiffer. Feedback stabilization of the two-dimensional Navier-Stokes equations by value function approximation. *Appl. Math. Optim.*, 80(3):599–641, 2019. doi:10.1007/s00245-019-09586-x.
- [17] P. Buchfink, S. Glas, and B. Haasdonk. Symplectic model reduction of Hamiltonian systems on nonlinear manifolds and approximation with weakly symplectic autoencoder. *SIAM J. Sci. Comput.*, 45(2):A289–A311, 2023. doi:10.1137/21M1466657.
- [18] T. Çimen. Survey of state-dependent Riccati equation in nonlinear optimal feedback control synthesis. *J. Guid. Control Dyn.*, 35(4):1025–1047, 2012. doi:10.2514/1.55821.
- [19] D.-A. Clevert, T. Unterthiner, and S. Hochreiter. Fast and accurate deep network learning by exponential linear units (ELUs). e-print 1511.07289, arXiv, 2015. Machine Learning (cs.LG). doi:10.48550/arXiv.1511.07289.
- [20] J. Darbon, G. P. Langlois, and T. Meng. Overcoming the curse of dimensionality for some Hamilton–Jacobi partial differential equations via neural network architectures. *Res. Math. Sci.*, 7(3):20, 2020. doi:10.1007/s40687-020-00215-6.
- [21] A. Das and J. Heiland. Low-order linear parameter varying approximations for nonlinear controller design for flows. e-print 2311.05305, arXiv, 2023. Optimization and Control (math.OC). doi:10.48550/arXiv.2311.05305.
- [22] S. J. Dodds. *Feedback Control: Linear, Nonlinear and Robust Techniques and Design with Industrial Applications*, chapter Sliding Mode Control and Its Relatives, pages 705–792. Advanced Textbooks in Control and Signal Processing. Springer, London, 2015. doi:10.1007/978-1-4471-6675-7_10.
- [23] S. Dolgov, D. Kalise, and K. Kunisch. Tensor decomposition methods for high-dimensional Hamilton-Jacobi-Bellman equations. *SIAM J. Sci. Comput.*, 43(3):A1625–A1650, 2021. doi:10.1137/19M1305136.
- [24] J. C. Dunn. A fuzzy relative of the isodata process and its use in detecting compact well-separated clusters. *Journal of Cybernetics*, 3(3):32–57, 1973. doi:10.1080/01969727308546046.
- [25] Maziar Moradi Fard, Thibaut Thonet, and Éric Gaussier. Deep k -means: Jointly clustering with k -means and learning representations. *Pattern Recognit. Lett.*, 138:185–192, 2020. doi:10.1016/J.PATREC.2020.07.028.

- [26] S. Fresca and A. Manzoni. POD-DL-ROM: Enhancing deep learning-based reduced order models for nonlinear parametrized PDEs by proper orthogonal decomposition. *Comput. Methods Appl. Mech. Eng.*, 388:114181, 2022. doi:10.1016/j.cma.2021.114181.
- [27] G. H. Golub and C. F. Van Loan. *Matrix Computations*. Johns Hopkins Studies in the Mathematical Sciences. Johns Hopkins University Press, Baltimore, fourth edition, 2013.
- [28] J. Heiland, P. Benner, and R. Bahmani. Convolutional neural networks for very low-dimensional LPV approximations of incompressible Navier-Stokes equations. *Front. Appl. Math. Stat.*, 8:879140, 2022. doi:10.3389/fams.2022.879140.
- [29] J. Heiland, Y. Kim, and S. W. R. Werner. Code, data and results for numerical experiments in “Deep polytopic autoencoders for low-dimensional linear parameter-varying approximations and nonlinear feedback design” (version 1.0), March 2024. doi:10.5281/zenodo.10783695.
- [30] J. Heiland and S. W. R. Werner. Low-complexity linear parameter-varying approximations of incompressible Navier-Stokes equations for truncated state-dependent Riccati feedback. *IEEE Control Syst. Lett.*, 7:3012–3017, 2023. doi:10.1109/LCSYS.2023.3291231.
- [31] Jan Heiland and Yongho Kim. Convolutional autoencoders, clustering, and POD for low-dimensional parametrization of flow equations. *Comput. Math. Appl.*, 175:49–61, 2024. doi:10.1016/j.camwa.2024.08.032.
- [32] Jan Heiland and Yongho Kim. Polytopic autoencoders with smooth clustering for reduced-order modeling of flows. *J. Comput. Phys.*, 521:113526, 2025. doi:10.1016/j.jcp.2024.113526.
- [33] Yu-Eop Kang, Soonho Shon, and Kwanjung Yee. Local non-intrusive reduced order modeling based on soft clustering and classification algorithm. *Int. J. Numer. Methods Eng.*, 123(10):2237–2261, 2022. doi:10.1002/nme.6934.
- [34] P. V. Kokotovic. The joy of feedback: nonlinear and adaptive. *IEEE Contr. Syst. Mag.*, 12(3):7–17, 1992. doi:10.1109/37.165507.
- [35] N. Lang, H. Mena, and J. Saak. An LDL^T factorization based ADI algorithm for solving large-scale differential matrix equations. *Proc. Appl. Math. Mech.*, 14(1):827–828, 2014. doi:10.1002/pamm.201410394.
- [36] Y. Lin and V. Simoncini. A new subspace iteration method for the algebraic Riccati equation. *Numer. Linear Algebra Appl.*, 22(1):26–47, 2015. doi:10.1002/nla.1936.
- [37] M. Ohlberger and S. Rave. Nonlinear reduced basis approximation of parameterized evolution equations via the method of freezing. *C. R. Math.*, 351(23–24):901–906, 2013. doi:10.1016/j.crma.2013.10.028.
- [38] S. Z. Rizvi, F. Abbasi, and J. M. Velni. Model reduction in linear parameter-varying models using autoencoder neural networks. In *2018 Annual American Control Conference (ACC)*, pages 6415–6420, 2018. doi:10.23919/ACC.2018.8431912.

- [39] J. Saak and S. W. R. Werner. Using LDL^T factorizations in Newton's method for solving general large-scale algebraic Riccati equations. e-print 2402.06844, arXiv, 2024. Numerical Analysis (math.NA). doi:10.48550/arXiv.2402.06844.
- [40] S. Shen, Y. Yin, T. Shao, H. Wang, C. Jiang, L. Lan, and K. Zhou. High-order differentiable autoencoder for nonlinear model reduction. *ACM Trans. Graph.*, 40(4):68, 2021. doi:10.1145/3450626.3459754.
- [41] E. D. Sontag. *Mathematical Control Theory*, volume 6 of *Texts in Applied Mathematics*. Springer, New York, second edition, 1998. doi:10.1007/978-1-4612-0577-7.
- [42] T. Stillfjord. Singular value decay of operator-valued differential Lyapunov and Riccati equations. *SIAM J. Control Optim.*, 56(5):3598–3618, 2018. doi:10.1137/18M1178815.
- [43] Miin-Shen Yang, Chien-Yo Lai, and Chih-Ying Lin. A robust em clustering algorithm for gaussian mixture models. *Pattern Recognit.*, 45(11):3950–3961, 2012. doi:10.1016/j.patcog.2012.04.031.